

Site-Specific Beam Learning for Full-Duplex Massive MIMO Wireless Systems

Samuel Li and Ian P. Roberts

Wireless Lab, Department of Electrical and Computer Engineering
University of California, Los Angeles (UCLA), Los Angeles, CA USA
Email: {samuel.li, ianroberts}@ucla.edu

Abstract—Existing beamforming-based full-duplex solutions for multi-antenna wireless systems often rely on explicit estimation of the self-interference channel. The pilot overhead of such estimation, however, can be prohibitively high in millimeter-wave and massive MIMO systems, thus limiting the practicality of existing solutions, especially in fast-fading conditions. In this work, we present a novel beam learning framework that bypasses explicit self-interference channel estimation by designing beam codebooks to efficiently obtain implicit channel knowledge that can then be processed by a deep learning network to synthesize transmit and receive beams for full-duplex operation. Simulation results using ray-tracing illustrate that our proposed technique can allow a full-duplex base station to craft serving beams that couple low self-interference while delivering high SNR, with 75–97% fewer measurements than would be required for explicit estimation of the self-interference channel.

Index Terms—Full-duplex, beamforming, self-interference, phased arrays, millimeter-wave, massive MIMO, deep learning.

I. INTRODUCTION

In-band full-duplex operation in future base stations has the potential to boost spectral efficiency, reduce latency, and enable advanced sensing capabilities, paving the way towards 6G wireless networks [1]. Realizing such full-duplex base stations requires effective suppression of the *self-interference* that arises when attempting to transmit and receive at the same time across the same frequency band, as the base station’s uplink signal could otherwise be severely degraded by its own downlink transmission and render full-duplex infeasible. In traditional sub-6 GHz wireless systems, self-interference cancellation has conventionally been performed through a combination of analog and digital cancellation techniques [2]–[4]. However, adapting these methods to millimeter-wave (mmWave) and massive multiple-input multiple-output (MIMO) base stations faces significant challenges due to their large antenna arrays, high operating frequencies, wide bandwidths, and hardware impairments [5], [6].

To address these challenges, recent work such as [7]–[11] has explored the use of beamforming to cancel self-interference, exploiting the high spatial degrees of freedom afforded by mmWave and massive MIMO transceivers. While these techniques show promise, most rely on an accurate estimate of the self-interference channel to design transmit and receive beams suitable for full-duplex operation. This can be problematic in real-world systems, since the dimensionality of the MIMO self-interference channel scales quadratically with

the number of antennas at the base station, which is typically on the order of tens or hundreds in the case of mmWave and massive MIMO. Barring sufficiently static channels, explicit estimation of the self-interference channel would therefore consume substantial pilot overhead, likely rendering it impractical in 5G/6G networks.

To our knowledge, the extent of existing research on full-duplex beam design without explicit self-interference channel knowledge is limited to [12]–[14]. The schemes in [12], [13] employ an exhaustive search over a small spatial grid, which can involve 50–500+ measurements per user pair, thus still incurring a significant overhead. In [14], a long short-term memory (LSTM) network is used to sequentially design a set of user-specific probing beams for implicit estimation of self-interference and of the downlink and uplink channels. The primary shortcoming of this approach is its poor scaling in multi-user scenarios, since the user-specific probing procedure necessitates additional feedback/coordination.

Taking inspiration from [15], [16], where site-specific codebooks are designed to reduce beam alignment overhead in half-duplex systems, we propose a novel beam learning framework that bypasses explicit self-interference channel estimation when designing beams to serve downlink and uplink in a full-duplex fashion. Our approach jointly optimizes a pair of transmit and receive probing codebooks for implicit self-interference channel estimation and a deep learning model that synthesizes the final serving beams. Notably, the user-agnostic nature of these probing beams allows the same implicit self-interference channel knowledge to be reused across many users, thereby minimizing the overhead of our solution. Simulations with ray-traced channel models demonstrate that our approach can design transmit and receive beams which approach the full-duplex capacity, while requiring only 3–25% of the measurements needed for explicit self-interference channel estimation.

II. SYSTEM MODEL

In this work, we consider a base station that aims to concurrently transmit to a downlink user while receiving from an uplink user on the same frequency resources. The base station is equipped with separate antenna arrays for transmission and reception, containing N_t and N_r antennas, respectively. Each antenna array is driven by a single radio frequency (RF) chain and analog beamforming weights to

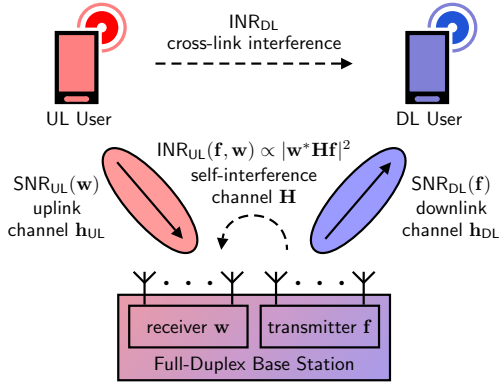


Fig. 1. An in-band full-duplex base station transmits to a downlink user while receiving from an uplink user across the same frequency band. This work aims to optimally design \mathbf{f} and \mathbf{w} without explicitly estimating \mathbf{H} .

dynamically steer beams, realized in hardware using an analog phase shifter and a variable attenuator at each antenna. Let us denote by $\mathbf{f} \in \mathbb{C}^{N_t \times 1}$ and $\mathbf{w} \in \mathbb{C}^{N_r \times 1}$ the transmit and receive beamforming weight vectors applied by the base station, each subject to a per-antenna power constraint as

$$|\mathbf{f}_i| \leq 1 \quad \forall i \in \{1, \dots, N_t\}, \quad (1)$$

$$|\mathbf{w}_j| \leq 1 \quad \forall j \in \{1, \dots, N_r\}. \quad (2)$$

Users are assumed to have a single omnidirectional antenna for simplicity, but this work readily extends to multi-antenna users. In serving any given downlink user, the base station transmits with power P_{DL} using its transmit beam \mathbf{f} across a channel $\mathbf{h}_{\text{DL}} \in \mathbb{C}^{N_t \times 1}$. Simultaneously, the base station receives from an uplink user, which transmits with power P_{UL} , across a channel $\mathbf{h}_{\text{UL}} \in \mathbb{C}^{N_r \times 1}$ using its receive beam \mathbf{w} . With this, we can express the downlink and uplink signal-to-noise ratios (SNRs) as

$$\text{SNR}_{\text{DL}}(\mathbf{f}) = \frac{P_{\text{DL}} |\mathbf{h}_{\text{DL}}^* \mathbf{f}|^2}{N_t \sigma_{\text{DL}}^2}, \quad (3)$$

$$\text{SNR}_{\text{UL}}(\mathbf{w}) = \frac{P_{\text{UL}} |\mathbf{w}^* \mathbf{h}_{\text{UL}}|^2}{\|\mathbf{w}\|_2^2 \sigma_{\text{UL}}^2}, \quad (4)$$

where σ_{DL}^2 and σ_{UL}^2 denote the per-antenna additive noise powers at each antenna on the downlink and uplink, respectively.

While operating in a full-duplex fashion, self-interference couples from the transmit array of the base station to its receive array across the MIMO self-interference channel $\mathbf{H} \in \mathbb{C}^{N_r \times N_t}$. The self-interference channel \mathbf{H} follows a Rician channel model as the sum of a line-of-sight (LOS) component \mathbf{H}_{LOS} and a non-line-of-sight (NLOS) component \mathbf{H}_{NLOS} , i.e.,

$$\mathbf{H} = \sqrt{\frac{\kappa}{\kappa+1}} \mathbf{H}_{\text{LOS}} + \sqrt{\frac{1}{\kappa+1}} \mathbf{H}_{\text{NLOS}}. \quad (5)$$

The LOS component is meant to capture near-field coupling between the base station's arrays, whereas the NLOS component represents reflections off nearby surroundings. While both components may fluctuate with time, the NLOS component is

likely to vary more quickly according to the dynamics of the environment in which the base station is deployed.

To quantify the severity of self-interference, we normalize its power by the noise floor, defining the interference-to-noise ratio (INR) at the base station receiver as

$$\text{INR}_{\text{UL}}(\mathbf{f}, \mathbf{w}) = \frac{P_{\text{DL}} |\mathbf{w}^* \mathbf{H} \mathbf{f}|^2}{N_t \|\mathbf{w}\|_2^2 \sigma_{\text{UL}}^2}. \quad (6)$$

Similar to INR_{UL} , the downlink user experiences cross-link interference from the uplink user's transmission, expressed as

$$\text{INR}_{\text{DL}} = \frac{P_{\text{UL}} |h|^2}{\sigma_{\text{DL}}^2}, \quad (7)$$

where $h \in \mathbb{C}$ is the channel from the uplink user to the downlink user. Treating self-interference as noise, the signal-to-interference-plus-noise ratios (SINRs) on the downlink and uplink are

$$\text{SINR}_{\text{DL}}(\mathbf{f}) = \frac{\text{SNR}_{\text{DL}}(\mathbf{f})}{1 + \text{INR}_{\text{DL}}}, \quad (8)$$

$$\text{SINR}_{\text{UL}}(\mathbf{f}, \mathbf{w}) = \frac{\text{SNR}_{\text{UL}}(\mathbf{w})}{1 + \text{INR}_{\text{UL}}(\mathbf{f}, \mathbf{w})}. \quad (9)$$

The achievable downlink and uplink spectral efficiencies are correspondingly

$$R_{\text{DL}}(\mathbf{f}) = \log_2(1 + \text{SINR}_{\text{DL}}(\mathbf{f})), \quad (10)$$

$$R_{\text{UL}}(\mathbf{f}, \mathbf{w}) = \log_2(1 + \text{SINR}_{\text{UL}}(\mathbf{f}, \mathbf{w})). \quad (11)$$

As a measure of overall performance of the full-duplex system, we sum the downlink and uplink spectral efficiencies as

$$R(\mathbf{f}, \mathbf{w}) = R_{\text{DL}}(\mathbf{f}) + R_{\text{UL}}(\mathbf{f}, \mathbf{w}), \quad (12)$$

which we seek to maximize in the next section through the design of \mathbf{f} and \mathbf{w} .

III. FULL-DUPLEX BEAM LEARNING

In this section, we present a novel approach to designing the transmit and receive beams (\mathbf{f} , \mathbf{w}) of the full-duplex base station in pursuit of maximizing sum spectral efficiency. A key distinction of our approach is in its use of deep learning to design these beams without explicitly estimating the self-interference channel $\mathbf{H} \in \mathbb{C}^{N_r \times N_t}$. This is in contrast to most prior work such as [7]–[9], [17], which require an accurate estimate of \mathbf{H} to design \mathbf{f} and \mathbf{w} . Such estimation can consume substantial pilot overhead, especially when \mathbf{H} changes frequently, e.g., due to dynamics in the environment.

Our proposed approach addresses this challenge by training a neural network $\mathcal{D}(\cdot)$ to synthesize near-optimal transmit and receive beams (\mathbf{f}^* , \mathbf{w}^*) using *implicit* knowledge of the self-interference channel. To optimize acquisition of such implicit channel knowledge, we jointly optimize the beam synthesizer $\mathcal{D}(\cdot)$ and a set of M pairs of transmit and receive beams $\{(\mathbf{f}_m, \mathbf{w}_m)\}_{m=1}^M$. These M pairs of probing beams collect $M \ll N_t N_r$ scalar measurements of self-interference across \mathbf{H} , which are then fed into the beam synthesizer, along with downlink/uplink channel knowledge, which we assume is acquired from conventional beam alignment or other channel state information mechanisms.

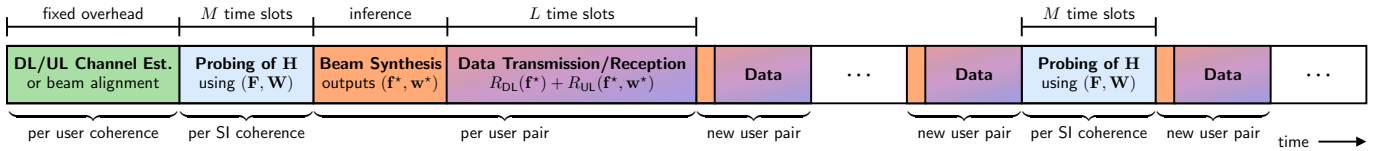


Fig. 2. Timeline of the envisioned use of our proposed scheme, with one time slot defined as the time to collect a single probing measurement across \mathbf{H} .

A. Envisioned Solution

The envisioned use of our proposed approach may take a variety of forms, one of which is illustrated in Fig. 2. In this scenario, the self-interference channel \mathbf{H} fades on a time scale faster than the user channels. As a result, downlink and uplink channel knowledge can be acquired relatively infrequently compared to probing of \mathbf{H} . In cases where \mathbf{H} is sufficiently stable, however, a single set of M probing measurements may be reused across a subset of user pairs, thereby saving on overhead.

Downlink and uplink channel acquisition: Our proposed framework begins by utilizing existing mechanisms for obtaining downlink and uplink channel knowledge, such as beam alignment in 5G networks [18]. In general, this channel knowledge can be either explicit estimates of \mathbf{h}_{DL} and \mathbf{h}_{UL} or implicit knowledge of some form, such as beam alignment measurements. As such, let us refer to it as simply \mathbf{y}_{DL} and \mathbf{y}_{UL} . Note that our approach will take as input downlink and uplink channel knowledge for a *single* user pair, but this channel knowledge may be collected beforehand for *all* user pairs the base station wishes to serve over some time horizon of interest. Naturally, this step would need to be repeated commensurate with the coherence time of the users' channels.

Probing of self-interference: The next component of our proposed scheme involves the base station collecting implicit knowledge of the self-interference channel \mathbf{H} through a series of M probing measurements. To collect the m -th probing measurement $z_m \in \mathbb{C}$, suppose the base station transmits with beam \mathbf{f}_m and receives using beam \mathbf{w}_m . Then, the received self-interference can be expressed as

$$z_m = \sqrt{\frac{P_{\text{DL}}}{N_t}} \mathbf{w}_m^* \mathbf{H} \mathbf{f}_m + \mathbf{w}_m^* \mathbf{n}_m, \quad (13)$$

where $\mathbf{n}_m \sim \mathcal{N}_{\mathbb{C}}(\mathbf{0}, \sigma_{\text{UL}}^2 \mathbf{I})$ denotes the complex Gaussian noise vector at the receive array during the m -th measurement.

Upon stacking the probing beams into matrices \mathbf{F} and \mathbf{W}

$$\mathbf{F} = [\mathbf{f}_1 \ \dots \ \mathbf{f}_M] \in \mathbb{C}^{N_t \times M} \quad (14)$$

$$\mathbf{W} = [\mathbf{w}_1 \ \dots \ \mathbf{w}_M] \in \mathbb{C}^{N_r \times M}, \quad (15)$$

the received signal vector $\mathbf{z} = [z_1 \ \dots \ z_M]^T \in \mathbb{C}^{M \times 1}$ can be expressed compactly as

$$\mathbf{z} = \sqrt{\frac{P_{\text{DL}}}{N_t}} \text{diag}(\mathbf{W}^* \mathbf{H} \mathbf{F}) + \text{diag}(\mathbf{W}^* \mathbf{N}), \quad (16)$$

with $\mathbf{N} \in \mathbb{C}^{N_r \times M}$ a matrix whose m -th column is \mathbf{n}_m . As will be clear shortly, the implicit channel knowledge contained in \mathbf{z} will be used to design the transmit and receive beams that

are used by the base station to serve the downlink and uplink users. Since explicit estimation of \mathbf{H} would in general require $N_t N_r$ measurements, we will seek $M \ll N_t N_r$ and, in this pursuit, will optimize \mathbf{F} and \mathbf{W} to extract information that is most useful in designing \mathbf{f} and \mathbf{w} .

Beam synthesis: With implicit knowledge of \mathbf{H} in hand, along with downlink and uplink channel knowledge, the last stage of our proposed approach is to synthesize the final serving beams. This is accomplished through a function $\mathcal{D}(\cdot)$, which takes as input \mathbf{z} , \mathbf{y}_{DL} , and \mathbf{y}_{UL} and outputs $(\mathbf{f}^*, \mathbf{w}^*) = \mathcal{D}(\mathbf{z}, \mathbf{y}_{\text{DL}}, \mathbf{y}_{\text{UL}})$.

B. Problem Formulation

Assembling together the components laid forth, our envisioned solution can be found by solving the following problem.

$$\max_{\mathbf{F}, \mathbf{W}, \mathcal{D}(\cdot)} \mathbb{E}_{\mathbf{H}, \mathbf{h}_{\text{DL}}, \mathbf{h}_{\text{UL}}} [R_{\text{DL}}(\mathbf{f}^*) + R_{\text{UL}}(\mathbf{f}^*, \mathbf{w}^*)] \quad (17a)$$

$$\text{s.t.} \quad (\mathbf{f}^*, \mathbf{w}^*) = \mathcal{D}(\mathbf{z}, \mathbf{y}_{\text{DL}}, \mathbf{y}_{\text{UL}}) \quad (17b)$$

$$\|\mathbf{f}^*\|_{\max}, \|\mathbf{w}^*\|_{\max} \leq 1 \quad (17c)$$

$$\|\mathbf{F}\|_{\max}, \|\mathbf{W}\|_{\max} \leq 1 \quad (17d)$$

Here, $\|\cdot\|_{\max} = \max_{i,j} |[\cdot]_{i,j}|$ denotes the max norm. Constraints (17b) and (17c) ensure that the synthesized serving beams $(\mathbf{f}^*, \mathbf{w}^*)$ and the probing codebooks (\mathbf{F}, \mathbf{W}) adhere to the per-antenna power constraints of (1) and (2). By maximizing the expectation of sum spectral efficiency, we aim to find a single design of \mathbf{F} , \mathbf{W} , and $\mathcal{D}(\cdot)$ that generalizes across user pairs and channel realizations. Solving problem (17) within the scope of an individual base station yields a *site-specific* solution which exploits the channel conditions at that particular site within the network.

C. Joint Probing Codebook Design and Beam Synthesis

To solve problem (17) and realize the envisioned solution, we propose a deep learning-based framework that jointly optimizes the probing codebooks (\mathbf{F}, \mathbf{W}) and the beam synthesizer $\mathcal{D}(\cdot)$ in an end-to-end manner. The overall architecture, depicted in Fig. 3, consists of trainable probing codebooks and a multi-layer neural network that parameterizes $\mathcal{D}(\cdot)$. Through unsupervised training, the model tailors \mathbf{F} and \mathbf{W} to gather channel information that is most useful to the beam synthesizer in its design of \mathbf{f}^* and \mathbf{w}^* to maximize the sum spectral efficiency. By training over the channel distributions of a single site, \mathbf{F} , \mathbf{W} , and $\mathcal{D}(\cdot)$ are all optimized to the particular base station at which they are deployed.

Recall, for \mathbf{F} and \mathbf{W} to be realizable in physical systems, they must be constrained to satisfy the per-antenna element

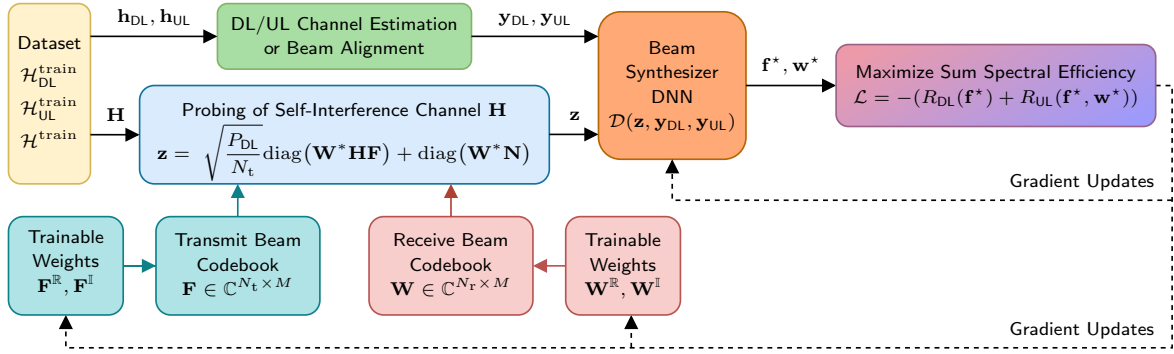


Fig. 3. Proposed end-to-end neural network model for full-duplex beam design.

magnitude limits given in (17c). However, directly optimizing the complex entries of \mathbf{F} and \mathbf{W} via gradient descent does not guarantee these constraints. Thus, we adopt an approach similar to [15], where the real and imaginary components of the codebooks are updated separately during training. After each update, the codebooks are projected element-wise to satisfy (17c), i.e.,

$$[\mathbf{F}]_{i,j} = \frac{[\mathbf{F}^{\mathbb{R}} + j\mathbf{F}^{\mathbb{I}}]_{i,j}}{\max(1, |[\mathbf{F}^{\mathbb{R}} + j\mathbf{F}^{\mathbb{I}}]_{i,j}|)}, \quad (18)$$

where $\mathbf{F}^{\mathbb{R}}$ and $\mathbf{F}^{\mathbb{I}}$ are the trainable weights that represent the real and imaginary parts of \mathbf{F} , respectively. \mathbf{W} is constructed similarly. We use this same projection to ensure that the serving beams \mathbf{f}^* and \mathbf{w}^* are physically realizable.

The entire model, encompassing the learnable codebooks (\mathbf{F}, \mathbf{W}) and the beam synthesizer network $\mathcal{D}(\cdot)$, is trained end-to-end on a dataset ($\mathcal{H}^{\text{train}}, \mathcal{H}_{\text{DL}}^{\text{train}}, \mathcal{H}_{\text{UL}}^{\text{train}}$) representative of the target operational environment. The objective is to maximize the expectation of the sum spectral efficiency defined in (12), which corresponds to minimizing the loss function

$$\mathcal{L} = -\mathbb{E}[R_{\text{DL}}(\mathbf{f}^*) + R_{\text{UL}}(\mathbf{f}^*, \mathbf{w}^*)]. \quad (19)$$

After training, the optimized codebooks \mathbf{F} and \mathbf{W} can be directly used by the base station to collect probing measurements \mathbf{z} according to (13). The trained beam synthesizer then uses these measurements to generate serving beams ($\mathbf{f}^*, \mathbf{w}^*$) for any given user pair. Once deployed, the only computational cost associated with our solution is that of beam synthesis $\mathcal{D}(\cdot)$, which amounts to inference through a neural network.

IV. NUMERICAL RESULTS

To evaluate our proposed method, we consider a 28 GHz base station whose transmitter and receiver are each equipped with a 4×4 half-wavelength uniform planar array and placed side by side, with their array centers separated by 10 wavelengths horizontally. To simulate the downlink and uplink channels, we use ray-tracing software [19] to deploy users around Dickson Plaza at UCLA and mount the base station atop Royce Hall, as illustrated in Fig. 4. Users are distributed within the field-of-view spanning -60° to 60° of the base

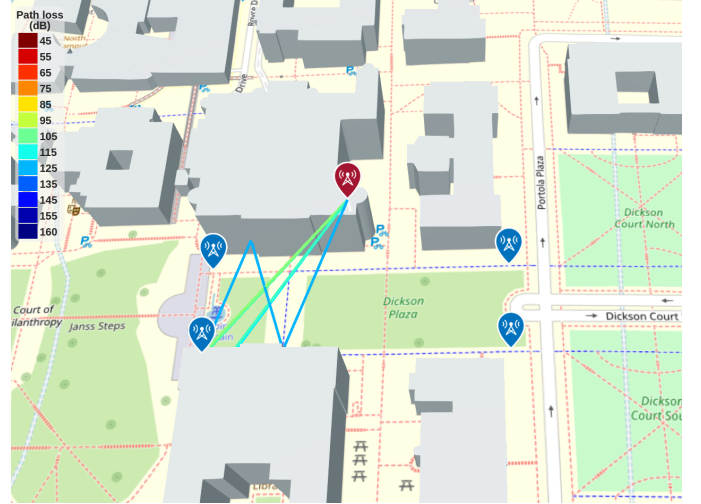


Fig. 4. Simulation scenario with a base station and multiple users. Users are arranged in an equidistant grid on the ground bounded by the blue markers, with the base station placed on a rooftop at the red marker. The traced rays for one user are visualized.

station, and the base station is down-tilted towards the center of the user distribution such that the median elevation is 0° .

The self-interference channel is modeled according to (5), where the LOS component \mathbf{H}_{LOS} is modeled as a spherical-wave channel [20], and the NLOS component \mathbf{H}_{NLOS} is comprised of a number of reflections off the environment. We consider both a finite number of reflections (each with amplitude drawn from a standard complex Gaussian) and an infinite number (i.e., Rayleigh fading). Since there are 16 antennas at the transmitter and receiver of the base station, the self-interference channel is of size 16×16 and therefore would in general require 256 scalar measurements to explicitly estimate.

At any given time, the base station aims to serve a pair of downlink and uplink users in a full-duplex fashion. While this is a predominantly LOS environment, there exist multiple NLOS paths to each user. We assume the base station conducts beam alignment to obtain knowledge of the LOS path (i.e., angle of departure/arrival) to each user; in this case, \mathbf{y}_{DL} and \mathbf{y}_{UL} are the LOS channel vectors to the users. The ignored

TABLE I
DEFAULT SIMULATION AND IMPLEMENTATION PARAMETERS

LOS component, \mathbf{H}_{LOS}	Spherical-wave channel [20]
NLOS component, \mathbf{H}_{NLOS}	Sum of 64 reflections
Self-interference Rician factor, κ	0 dB
Maximum downlink and uplink SNR	10 dB
Maximum INR	40 dB
Number of neurons in each layer of $\mathcal{D}(\cdot)$	$[16, 16, 8, 8] \times (N_t + N_r)$

NLOS components thus represent downlink/uplink channel estimation error. To normalize the performance evaluation, we scale \mathbf{h}_{DL} , \mathbf{h}_{UL} , and \mathbf{H} so that the maximum downlink and uplink SNR specified in (3) and (4) are equal to 10 dB and the maximum INR in (6) is 40 dB. We ignore cross-link interference INR_{DL} to focus solely on the effects of self-interference at the base station.

The probing codebooks are implemented according to (18), and the beam synthesizer is parameterized by a fully connected neural network that takes the concatenated vector $(\mathbf{z}, \mathbf{y}_{\text{DL}}, \mathbf{y}_{\text{UL}})$ as input, with 4 hidden layers and the number of neurons in each layer scaled based on N_t and N_r , as shown in Table I. The model is trained end-to-end with a batch size of 4096 using Adam optimizer. A learning rate of 0.001 is used for the beam synthesizer, and a learning rate of 0.0015 is used for the codebooks in conjunction with a cosine annealing scheduler with a period of 5000 batches and a minimum learning rate of 0.0005. The model is trained until convergence before being tested against 20,000 unseen channel realizations to evaluate its performance. The default parameters used in simulations are summarized in Table I, unless specified otherwise.

We compare the performance of our model against (i) maximum ratio transmission (MRT) and maximum ratio combining (MRC) using estimated downlink and uplink channels, and (ii) the full-duplex capacity, taken as the sum of the downlink and uplink capacity, which can only be achieved by MRT+MRC with perfect downlink and uplink channel knowledge in the absence of self-interference.

First, we investigate the impact of the self-interference channel conditions on the sum spectral efficiency by varying the Rician factor κ , as shown in Fig. 5. With only 8–64 measurements of self-interference, we can see appreciable performance across κ , which confirms that our approach is indeed able to perform well with a fraction of the measurements needed for explicit estimation of \mathbf{H} . We can also observe that our model provides improved sum spectral efficiency as κ increases. This cannot be attributed to favorable self-interference conditions, as the MRT+MRC baseline trends in the opposite direction. Instead, as the self-interference channel becomes dominated by the LOS component under high κ , the channel becomes more deterministic. As a result, the model is able to infer a more accurate channel representation, leading to improved performance. Conversely, in the low- κ regime, where the self-interference channel becomes more stochastic, additional probing measurements yield more pronounced gains

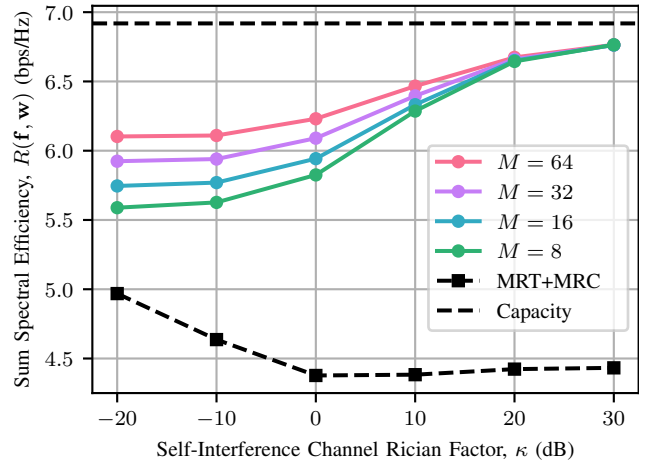


Fig. 5. Sum spectral efficiency as a function of the self-interference channel Rician factor κ for various numbers of probing measurements M , where the number of reflections in \mathbf{H}_{NLOS} is 64 and \mathbf{H}_{LOS} is the spherical-wave model.

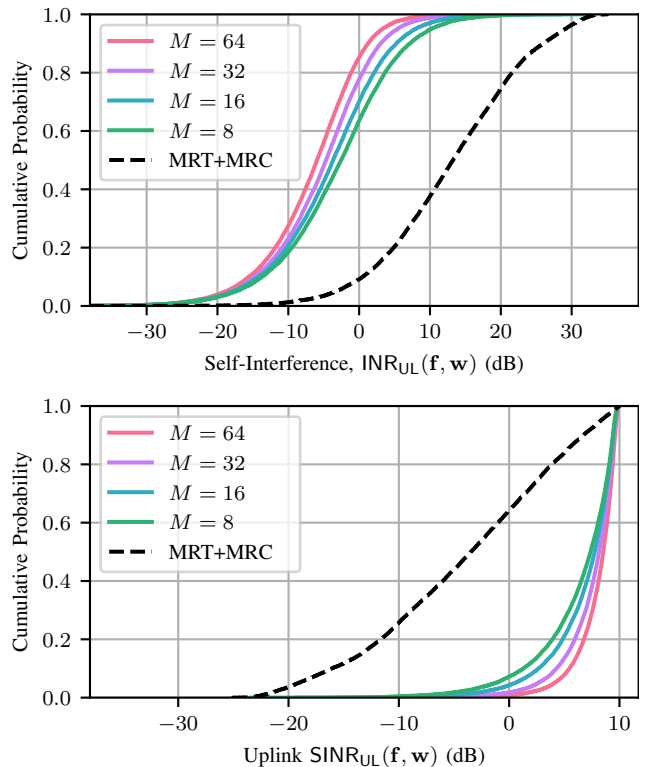


Fig. 6. CDFs of (a) self-interference INR_{UL} and (b) uplink SINR_{UL} for different numbers of probing measurements M , where $\kappa = 0$ dB.

in sum spectral efficiency.

Further evaluating the impact of M on the model's performance, Fig. 6 displays the cumulative distribution functions (CDFs) of INR_{UL} and SINR_{UL} for different numbers of probing measurements M . The MRT+MRC baseline incurs approximately 15 dB of INR, which severely degrades SINR and renders full-duplex operation infeasible. In contrast, our model achieves an INR reduction of nearly 20 dB with only $M = 16$ probing beams, reducing self-interference to below

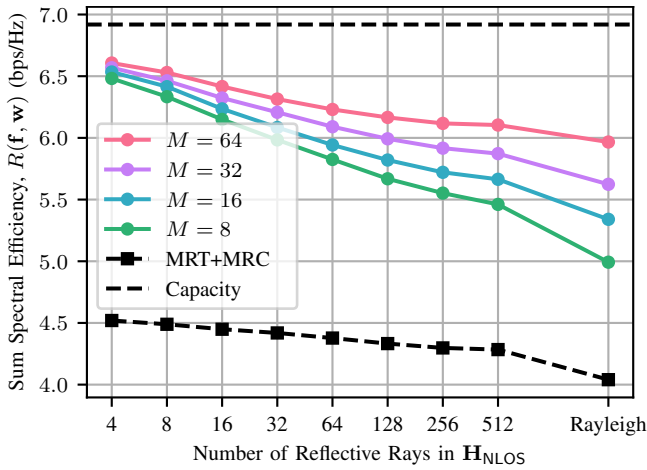


Fig. 7. Sum spectral efficiency as a function of the number of reflective rays in the NLOS component of the self-interference channel for different numbers of probing beams M , where $\kappa = 0$ dB.

the noise floor the majority of the time and increasing uplink SINR significantly—a trend that continues with more measurements. This demonstrates our model’s ability to effectively mitigate self-interference with a limited number of probing beams, offering a favorable trade-off between performance and measurement overhead.

In Fig. 7, we train and test our model across different self-interference channel configurations by varying the number of reflections in the NLOS component \mathbf{H}_{NLOS} . This is particularly relevant to consider because only the NLOS portion of self-interference meaningfully changes with time, making the estimation of this component the principal role of probing. With fewer rays, fewer probing measurements M are needed to attain high sum spectral efficiency and increasing the number of probing measurements offers little gain. As the number of rays increases, the benefit of more measurements appears, especially when an infinite number of rays are present in the case of Rayleigh fading. However, in such regimes, the self-interference channel is particularly rich, making it difficult to reliably obtain enough implicit knowledge from only $M = 64$ measurements, considering the channel matrix is full rank of size 16×16 .

V. CONCLUSION

This work develops a novel beam learning framework for full-duplex base stations that aims to achieve high sum spectral efficiency while minimizing the number of probing beams required for self-interference channel estimation. This is realized by designing site-specific probing codebooks to implicitly estimate the self-interference channel and then synthesizing the final downlink and uplink beams using a deep learning model. Our approach is in stark contrast to many existing schemes, whose reliance on explicit estimation of the self-interference channel would incur prohibitive overhead in most real-world settings. We demonstrate that our approach can suppress self-interference to near or below the noise floor and attain high sum spectral efficiency with only 8–64 probing

measurements, even when the self-interference channel itself contains 256 unknown elements. Numerical results using ray-tracing also illustrates our model’s robustness to varying channel conditions. Valuable future work may explore how to extend ideas herein to multi-user systems or may experimentally demonstrate beam learning schemes using actual wireless platforms.

ACKNOWLEDGMENTS

This work used computational and storage services from the Hoffman2 Cluster, operated by the UCLA Office of Advanced Research Computing’s Research Technology Group.

REFERENCES

- [1] B. Smida *et al.*, “Full-duplex wireless for 6G: Progress brings new opportunities and challenges,” *IEEE J. Sel. Areas Commun.*, vol. 41, no. 9, pp. 2729–2750, Sep. 2023.
- [2] A. Sabharwal *et al.*, “In-band full-duplex wireless: Challenges and opportunities,” *IEEE J. Sel. Areas Commun.*, vol. 32, no. 9, pp. 1637–1652, Sep. 2014.
- [3] K. E. Kolodziej, B. T. Perry, and J. S. Herd, “In-band full-duplex technology: Techniques and systems survey,” *IEEE Trans. Microw. Theory Techn.*, vol. 67, no. 7, pp. 3025–3041, Feb. 2019.
- [4] J. Kim *et al.*, “On the learning of digital self-interference cancellation in full-duplex radios,” *IEEE Wireless Commun.*, vol. 31, no. 4, pp. 184–191, Aug. 2024.
- [5] B. Smida *et al.*, “In-band full-duplex: The physical layer,” *Proc. IEEE*, vol. 112, no. 5, pp. 433–462, May 2024.
- [6] I. P. Roberts, J. G. Andrews, H. B. Jain, and S. Vishwanath, “Millimeter-wave full duplex radios: New challenges and techniques,” *IEEE Wireless Commun.*, vol. 28, no. 1, pp. 36–43, Feb. 2021.
- [7] S. Huang, Y. Ye, and M. Xiao, “Learning-Based Hybrid Beamforming Design for Full-Duplex Millimeter Wave Systems,” *IEEE Trans. Cogn. Commun. Netw.*, vol. 7, no. 1, pp. 120–132, Mar. 2021.
- [8] I. P. Roberts, S. Vishwanath, and J. G. Andrews, “LONESTAR: Analog beamforming codebooks for full-duplex millimeter wave systems,” *IEEE Trans. Wireless Commun.*, vol. 22, no. 9, pp. 5754–5769, Sep. 2023.
- [9] R. Hernangómez, J. Fink, R. L. G. Cavalcante, and S. Stańczak, “CISSIR: Beam Codebooks with Self-Interference Reduction Guarantees for Integrated Sensing and Communication Beyond 5G,” Feb. 2025.
- [10] I. Bilbao *et al.*, “Deep Unfolding-Powered Analog Beamforming for In-Band Full-Duplex,” *IEEE Open J. Commun. Soc.*, vol. 5, pp. 3753–3761, 2024.
- [11] R. López-Valcarce and M. Martínez-Cotelo, “Full-duplex mmWave MIMO with finite-resolution phase shifters,” *IEEE Trans. Wireless Commun.*, vol. 21, no. 11, pp. 8979–8994, Nov. 2022.
- [12] I. P. Roberts, A. Chopra, T. Novlan, S. Vishwanath, and J. G. Andrews, “STEER: Beam selection for full-duplex millimeter wave communication systems,” *IEEE Trans. Commun.*, vol. 70, no. 10, pp. 6902–6917, 2022.
- [13] I. P. Roberts, Y. Zhang, T. Osman, and A. Alkhateeb, “STEER+: Robust beam refinement for full-duplex millimeter wave communication systems,” in *Proc. Asilomar Conf. Signals, Sys., and Comput.*, Oct. 2023.
- [14] J. M. Kong and I. P. Roberts, “Active beam learning for full-duplex wireless systems,” in *Proc. Asilomar Conf. Signals Sys. Comput.*, Oct. 2024.
- [15] Y. Heng and J. G. Andrews, “Grid-Free MIMO Beam Alignment Through Site-Specific Deep Learning,” *IEEE Trans. Wireless Commun.*, vol. 23, no. 2, pp. 908–921, Feb. 2024.
- [16] Y. Zhang, M. Alrabeiah, and A. Alkhateeb, “Reinforcement learning of beam codebooks in millimeter wave and terahertz MIMO systems,” *IEEE Trans. Commun.*, vol. 70, no. 2, pp. 904–919, Nov. 2022.
- [17] J. Palacios, J. Rodríguez-Fernández, and N. González-Prelcic, “Hybrid precoding and combining for full-duplex millimeter wave communication,” in *Proc. IEEE GLOBECOM*, Dec. 2019, pp. 1–6.
- [18] Y. Heng *et al.*, “Six key challenges for beam management in 5.5G and 6G systems,” *IEEE Commun. Mag.*, vol. 59, no. 7, pp. 74–79, Jul. 2021.
- [19] T. M. Inc., “Communications toolbox version: 24.2 (R2024b),” The MathWorks Inc., 2024.
- [20] J.-S. Jiang and M. A. Ingram, “Spherical-wave model for short-range MIMO,” *IEEE Trans. Commun.*, vol. 53, no. 9, pp. 1534–1541, 2005.